Please cite this article in press as: Jaraíz-Rodríguez et al., A Short Region of Connexin43 Reduces Human Glioma Stem Cell Migration, Invasion, and Survival through Src, PTEN, and FAK, Stem Cell Reports (2017), http://dx.doi.org/10.1016/j.stemcr.2017.06.007

Stem Cell Reports
Article

ISSCR

OPEN ACCESS

A Short Region of Connexin43 Reduces Human Glioma Stem Cell Migration, Invasion, and Survival through Src, PTEN, and FAK

Myriam Jaraíz-Rodríguez,[1] Ma Dolores Tabernero,[2,3] María González-Tablas,[2,3] Alvaro Otero,[4] Alberto Orfao,[3] Jose M. Medina,[1] and Arantxa Tabernero[1,*]

[1]Instituto de Neurociencias de Castilla y León (INCYL), Departamento de Bioquímica y Biología Molecular, Universidad de Salamanca, C/ Pintor Fernando Gallego 1, 37007 Salamanca, Spain

[2]Instituto de Estudios de Ciencias de la Salud de Castilla y León (IECSCYL), Instituto de Investigación Biomédica de Salamanca (IBSAL), 37007 Salamanca, Spain

[3]Centre for Cancer Research (CIC-IBMCC; CSIC/USAL; IBSAL), Departamento de Medicina Universidad de Salamanca, 37007 Salamanca, Spain

[4]Neurosurgery Service, Hospital Universitario de Salamanca and IBSAL, 37007 Salamanca, Spain

*Correspondence: ataber@usal.es

http://dx.doi.org/10.1016/j.stemcr.2017.06.007

SUMMARY

Connexin43 (CX43), a protein that forms gap junction channels and hemichannels in astrocytes, is downregulated in high-grade gliomas. Its relevance for glioma therapy has been thoroughly explored; however, its positive effects on proliferation are counterbalanced by its effects on migration and invasion. Here, we show that a cell-penetrating peptide based on CX43 (TAT-Cx43$_{266-283}$) inhibited c-Src and focal adhesion kinase (FAK) and upregulated phosphatase and tensin homolog in glioma stem cells (GSCs) derived from patients. Consequently, TAT-Cx43$_{266-283}$ reduced GSC motility, as analyzed by time-lapse microscopy, and strongly reduced their invasive ability. Interestingly, we investigated the effects of TAT-Cx43$_{266-283}$ on freshly removed surgical specimens as undissociated glioblastoma blocks, which revealed a dramatic reduction in the growth, migration, and survival of these cells. In conclusion, a region of CX43 (amino acids 266–283) exerts an important anti-tumor effect in patient-derived glioblastoma models that includes impairment of GSC migration and invasion.

RESULTS

INTRODUCTION

Connexin43 (CX43) is an integral membrane protein that is widely expressed in astrocytes (Giaume et al., 2010) and is downregulated in high-grade gliomas, the most common malignant tumor of the CNS (Crespin et al., 2016; Huang et al., 1999; Pu et al., 2004; Shinoura et al., 1996; Soroceanu et al., 2001). Patients diagnosed with glioblastoma multiforme, the most aggressive form of glioma, have a median survival rate of 1–2 years (Gilbert et al., 2014) because of the infiltrative nature of these tumors, which facilitates recurrence after surgery and standard therapy. These tumors are composed of a heterogeneous population of cells, including many with stem cell-like properties, called glioma-initiating cells or glioma stem cells (GSCs). GSCs are characterized by their self-renewal capacity, high oncogenic potential, resistance to standard therapies (Chen et al., 2012; Dirks, 2010), and high invasive capacity (Cheng et al., 2011; Garcia et al., 2010).

GSCs express very low levels of CX43. When this protein is restored, the stem cell phenotype of GSC lines is reversed and their tumorigenicity is reduced (Gangoso et al., 2014; Yu et al., 2012). Our previous studies revealed that CX43 exerts this effect through the inhibition of c-Src activity. Thus, restoring CX43 inhibited the oncogenic activity of c-Src in different glioma cell lines (Gangoso et al., 2014; Gonzalez-Sanchez et al., 2016; Herrero-Gonzalez et al., 2010). Inhibition of c-Src is caused by a short region, residues 266–283, within the C-terminal domain of CX43 that recruits c-Src together with its inhibitors, C-terminal Src kinase (CSK) and phosphatase and tensin homolog (PTEN) (Gonzalez-Sanchez et al., 2016). In fact, cell-penetrating peptides containing the CX43 residues 266–283 (TAT-Cx43$_{266-283}$) are able to mimic these effects. Indeed, as a result of c-Src inhibition, TAT-Cx43$_{266-283}$ increased PTEN, with subsequent inactivation of AKT (Gonzalez-Sanchez et al., 2016), downregulated the expression of the inhibitor of differentiation (ID1), and the transcription factor, SOX-2, and promoted cadherin switching (Gangoso et al., 2014) in the GSC lines GliNS2 and G166. Consequently, the ability of GlinNS2 and G166 GSCs to proliferate and generate neurospheres decreased and the percentage of cells expressing differentiation markers increased in the presence of TAT-Cx43$_{266-283}$ (Gangoso et al., 2014; Gonzalez-Sanchez et al., 2016).

One important substrate of c-Src is focal adhesion kinase (FAK). c-Src binds to FAK and phosphorylates the tyrosine residues 576 and 577 in the activation loop of FAK (Calalb et al., 1995), thereby maximizing its kinase activity and creating additional protein binding sites (Mitra and Schlaepfer, 2006). This active FAK-Src complex stimulates the activity of RAC1 and CDC42 to increase membrane protrusions and mediates the transient suppression of RHOA-GTP levels, thereby facilitating cell spreading. Not surprisingly, both *Src*–/– and FAK (*Ptk2*)–/– fibroblasts display impaired migration (Ilić et al., 1995; Klinghoffer et al., 1999). c-Src and FAK are required for the processes of cell invasion and migration in tumor cells (Carragher

Please cite this article in press as: Jaraíz-Rodríguez et al., A Short Region of Connexin43 Reduces Human Glioma Stem Cell Migration, Invasion, and Survival through Src, PTEN, and FAK, Stem Cell Reports (2017), http://dx.doi.org/10.1016/j.stemcr.2017.06.007

et al., 2006; van Nimwegen et al., 2005), including glioblastoma (Du et al., 2009; Lindemann et al., 2011) and GSCs (Frolov et al., 2016; Liu et al., 2016). In fact, the activity of both c-Src and FAK are augmented in glioblastomas (Riemenschneider et al., 2005; Zhang et al., 2011). In addition, PTEN, as a tyrosine phosphatase, interacts directly with and dephosphorylates FAK (Cai et al., 2005; Tamura et al., 1998), leading to suppression of glioma cell migration and invasion (Park et al., 2002).

As previously mentioned, the major obstacle to developing a cure for glioblastoma is its diffuse invasion property, which enables GSCs to escape complete surgical resection, chemotherapy, and radiation therapy. Therefore, an important therapeutic aim is to reduce GSC motility and invasion. Because TAT-Cx43$_{266-283}$ inhibits c-Src activity and upregulates PTEN, in this study, we investigated whether TAT-Cx43$_{266-283}$ reduces FAK activity with subsequent impairment in GSC motility and invasive capacity.

RESULTS

TAT-Cx43$_{266-283}$ Inhibits c-Src Activity and Upregulates PTEN in Primary Glioblastoma Stem Cells

Our previous studies showed that cell-penetrating peptides containing the residues of CX43 involved in the interaction with c-Src (residues 266–283) fused to the TAT-penetrating sequence (TAT-Cx43$_{266-283}$) inhibit c-Src activity in the human GSC lines GliNS2 and G166 (Gangoso et al., 2014; Gonzalez-Sanchez et al., 2016). In this study, we investigated whether this effect also occurs in GSCs derived directly from patients (primary GSCs). To do so, primary GSCs were obtained and cultured from human glioblastoma biopsies immediately after surgery, as described previously (Pollard et al., 2009; Thirant et al., 2011). As expected, most of the cells in these cultures expressed the stem cell markers SOX-2 and Nestin (Figures 1A and S1). The c-Src activity was analyzed by measuring the levels of c-Src phosphorylated at Tyr416 (Y416 c-Src), the active form of this tyrosine kinase (Kmiecik and Shalloway, 1987). Our results showed that the level of activated c-Src decreased after 24 hr of incubation with 50 μM TAT-Cx43$_{266-283}$ compared with cells incubated with 50 μM TAT-penetrating peptide (TAT) or with control (Figures 1B and 1C) in primary GSCs derived from five glioblastoma patients (G9, G12, G13, G15, and G16). These results indicate that TAT-Cx43$_{266-283}$ inhibits c-Src activity also in primary GSCs.

As a result of c-Src inhibition, TAT-Cx43$_{266-283}$ increases PTEN, with subsequent AKT inactivation and a reduction in G166 GSC proliferation and survival (Gonzalez-Sanchez et al., 2016). Because PTEN is one of the most relevant tumor suppressor proteins in gliomas (Cancer Genome Atlas Research Network, 2008), in this study, we analyzed the effect of TAT-Cx43$_{266-283}$ on PTEN in primary GSCs. Our data revealed that TAT-Cx43$_{266-283}$ upregulated the PTEN levels in these primary GSCs (Figures 1B and 1D).

TAT-Cx43$_{266-283}$ Targets FAK

FAK autophosphorylation at Tyr397 (Y397 FAK) creates a binding site for c-Src that phosphorylates FAK at Tyr576 (Y576 FAK) and Tyr577 (Y577 FAK), promoting maximal FAK catalytic activity. In fact, FAK phosphorylation at Y576 and Y577 is required for maximal Y397 phosphorylation (Ruest et al., 2000). In addition, PTEN dephosphorylates Y397 FAK, which decreases FAK activity (Tamura et al., 1998). Therefore, in this study, we investigated whether changes in the c-Src activity and PTEN levels promoted by TAT-Cx43$_{266-283}$ impact FAK activity in GSCs.

Our results showed that, except for G12 GSCs, in which changes were not statistically significant, incubation with 50 μM TAT-Cx43$_{266-283}$ for 24 hr decreased the Y397 FAK phosphorylation levels compared with incubation with TAT or control in primary GSCs (Figures 1B and 1E).

We also analyzed the effect of TAT-Cx43$_{266-283}$ on FAK residues that were directly phosphorylated by c-Src (Y576 and Y577). Figure 2A shows that primary G9 GSCs incubated with 25 or 50 μM TAT-Cx43$_{266-283}$ for 15 hr had lower levels of Y576 and Y577 FAK compared with those incubated with the same TAT concentrations. In fact, as soon as 4 hr after 50 μM TAT-Cx43$_{266-283}$ incubation, the c-Src activity decreased in primary GSCs, although no changes in FAK phosphorylation were found (Figure S2). However, 2 hr later, i.e., 6 hr after incubation with 50 μM TAT-Cx43$_{266-283}$, both the c-Src activity and FAK phosphorylation levels decreased compared with the TAT treatment (Figure S2), suggesting that inhibition of c-Src activity leads to a reduction in FAK phosphorylation. Similarly, FAK phosphorylation at Y576 and Y577 was reduced by TAT-Cx43$_{266-283}$ in G166 GSCs (Figure 2B), a cell line in which the anti-tumor effect of TAT-Cx43$_{266-283}$ has been shown to be caused by c-Src inhibition (Gonzalez-Sanchez et al., 2016).

TAT-Cx43$_{266-283}$ Reduces GSC Motility

FAK plays a key role in both normal and tumor cell migration downstream of growth factor and integrin receptors (McLean et al., 2005). Because TAT-Cx43$_{266-283}$ inhibits FAK activity (Figures 1B, 1E, and 2), we investigated the effect of TAT-Cx43$_{266-283}$ on GSC migration. Primary G9, G13, G16, or G166 GSCs were exposed to TAT or TAT-Cx43$_{266-283}$ for 15 hr, and their movements were followed by time-lapse microscopy (representative movies are shown as Movies S1, S2, and S3). These movies show that 50 μM TAT-Cx43$_{266-283}$ greatly reduced cell motility in primary G9 GSCs (Movie S3) compared with the

Please cite this article in press as: Jaraíz-Rodríguez et al., A Short Region of Connexin43 Reduces Human Glioma Stem Cell Migration, Invasion, and Survival through Src, PTEN, and FAK, Stem Cell Reports (2017), http://dx.doi.org/10.1016/j.stemcr.2017.06.007

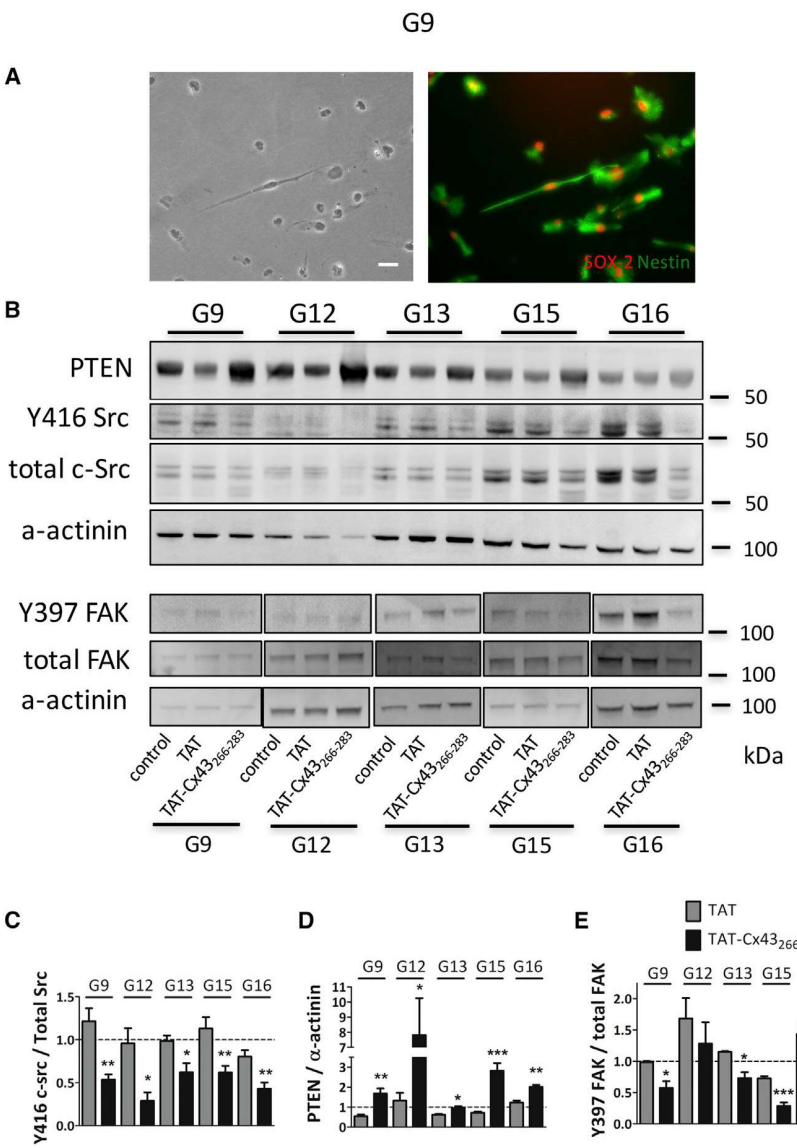

Figure 1. TAT-Cx43$_{266-283}$ Targets c-Src, PTEN, and FAK in Primary GSCs

(A) Phase-contrast images (left) and SOX-2 (red) and Nestin (green) immunostaining (right) of the same field showing that primary G9 GSCs express these GSC markers. Scale bar, 50 μm.

(B) Primary G9, G12, G13, G15, and G16 GSCs were incubated with 50 μM TAT or 50 μM TAT-Cx43$_{266-283}$. After 24 hr, the PTEN, total c-Src, Y416 c-Src, total FAK, and Y397 FAK levels were analyzed by western blotting.

(C–E) Quantification of the Y416 c-Src/total c-Src (C), PTEN/α-actinin (D), and Y379 FAK/total FAK (E) ratios. The results were normalized with their corresponding controls (assigned a value of 1; dotted line) and are the means ± SEM of at least three independent experiments (ANOVA; ***$p < 0.001$, **$p < 0.01$, *$p < 0.05$; TAT-Cx43$_{266-283}$ versus TAT). See also Figure S1.

corresponding concentrations of TAT (Movie S2) or with the control (Movie S1). To quantify these effects, individual cell trajectories were tracked. Our results clearly show that the trajectories described for 12–14 hr by G166 GSCs (Figure 3A) and primary G9, G13, and G16 GSCs (Figures 3C, 4A, and 4C), were shorter when they were exposed to 25 or 50 μM TAT-Cx43$_{266-283}$ compared with TAT or control. Indeed, TAT-Cx43$_{266-283}$, at concentrations ranging from 25 to 50 μM, caused a significant reduction in the path length described by both G166 and primary GSCs (Figures 3B, 3D, 4B, and 4D).

To test whether these effects were carried out specifically by TAT-Cx43$_{266-283}$, we checked the effect of the 274–291 CX43 sequence fused to TAT (TAT-Cx43$_{274-291}$). It should be mentioned that the 274–291 CX43 sequence does not recruit c-Src together with its inhibitors, PTEN and CSK (Gonzalez-Sanchez et al., 2016), and consequently does not reduce Src activity with the subsequent reversion of the GSC phenotype in GliNS2 GSCs (Gangoso et al., 2014). Our results showed that TAT-Cx43$_{274-291}$ did not significantly modify the length of the primary G13 and G16 GSC trajectories (Figures 4B and 4D). To confirm the participation of FAK in the mechanism by which TAT-Cx43$_{266-283}$ reduced GSC motility, FAK activity was inhibited with 5 μM FAK inhibitor 14. Figures 4B and 4D reveal that G13 and G16 GSC motility was strongly reduced by the FAK inhibitor compared with the control, indicating that FAK activity is required for GSC motility.

Please cite this article in press as: Jaraíz-Rodríguez et al., A Short Region of Connexin43 Reduces Human Glioma Stem Cell Migration, Invasion, and Survival through Src, PTEN, and FAK, Stem Cell Reports (2017), http://dx.doi.org/10.1016/j.stemcr.2017.06.007

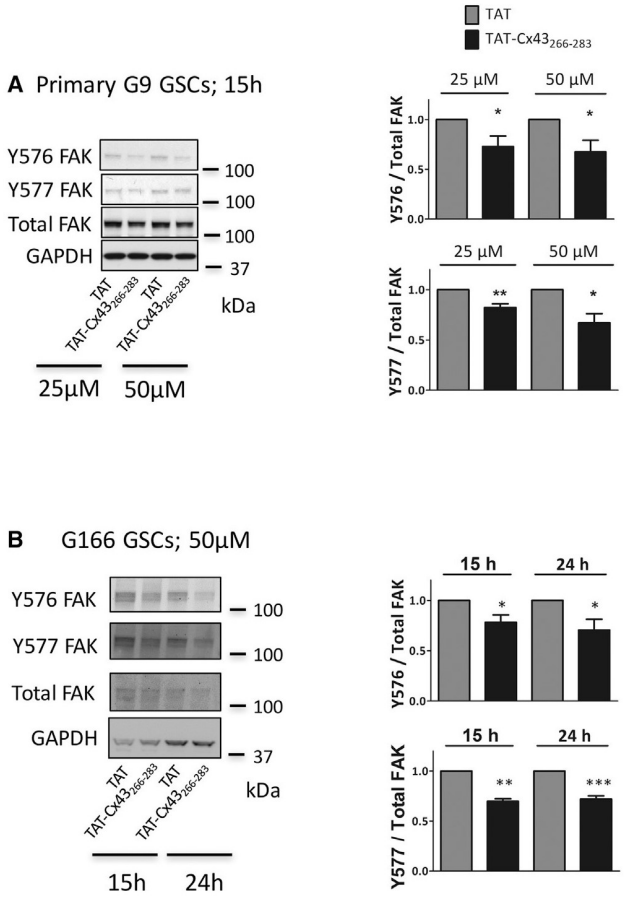

Figure 2. TAT-Cx43$_{266-283}$ Reduces Y576 and Y577 FAK Phosphorylation in GSCs

Primary G9 (A) or G166 (B) GSCs were incubated with TAT or TAT-Cx43$_{266-283}$. Western blot analysis for FAK, Y576 FAK, and Y577 FAK. The results were normalized with their corresponding TAT (assigned a value of 1) and are the means ± SEM of at least four independent experiments (***p < 0.001, **p < 0.01, *p < 0.05; TAT-Cx43$_{266-283}$ versus TAT, t test). See also Figure S2.

In fact, the effect of FAK inhibitor 14 plus TAT-Cx43$_{266-283}$ did not affect or slightly increased this effect compared with the FAK inhibitor alone (Figures 4B and 4D), suggesting that Src-dependent pathways other than FAK have a minor contribution to the effect of TAT-Cx43$_{266-283}$ on migration.

TAT-Cx43$_{266-283}$ Reduces GSC Invasion

Because TAT-Cx43$_{266-283}$ affects c-Src, PTEN, and FAK, three proteins that share common pathways to promote tumor cell invasion, we further hypothesized that TAT-Cx43$_{266-283}$ could decrease the invasive capacity of GSCs. To address this point, cultures of primary G9 or G166 GSCs were established in a Matrigel transwell system. Matrigel is an assortment of extracellular matrix proteins, mainly laminin, collagen IV, and enactin, and it is considered to be a reconstituted basement membrane preparation (Hughes et al., 2010). Matrigel occludes transwell membrane pores, blocking non-invasive cells from migrating through. In contrast, invasive cells can degrade the matrix and move through the extracellular layer and adhere to the bottom of the transwell.

Typical fields obtained from the bottom of transwells after 15 hr of Matrigel invasion, as shown in Figure 5, show that the ability of the cells to invade the basement membrane was significantly compromised in TAT-Cx43$_{266-283}$-treated primary G9 and G166 GSCs (Figures 5A and 5B) relative to TAT-treated cells. When quantifying these results, we observed that TAT-Cx43$_{266-283}$ decreased the invasion capacity of the primary G9 and G166 GSCs by approximately 63%–66% and 34%–37%, respectively, relative to TAT-treated cells. It should be mentioned that TAT, even at 100 μM, only slightly (11% in primary G9 GSCs) modified or did not modify the invasive ability of these cells compared with the control (Figure S3). In addition, the observed reduction in the number of invading cells was not due to a decrease in cell proliferation or cytotoxicity, because TAT-Cx43$_{266-283}$ applied at such concentrations (up to 50 μM) for 15 hr did not affect or only slightly affected (9% and 13% in G9 at 25 and 50 μM, respectively; TAT-Cx43$_{266-283}$ versus TAT) the viability of primary G9 and G166 GSCs (Figures S4A and S4B).

TAT-Cx43$_{266-283}$ Dramatically Reduced Growth, Migration, and Survival of Glioblastoma Cells from Freshly Removed Surgical Malignant Glioma Specimens

To test the effect of TAT-Cx43$_{266-283}$ on GSC migration and invasion, concentrations ranging from 25 to 50 μM for 15 hr were chosen to avoid the effects related to GSC viability (Figures S4A–S4D). TAT-Cx43$_{266-283}$ inhibits the oncogenic activity of c-Src, which in addition to its effect on migration is involved in a diverse spectrum of cancer tumor events, including the stem cell phenotype, survival, differentiation, or proliferation (Zhang et al., 2011). In fact, Figures S4E and S4F and our previous studies show that TAT-Cx43$_{266-283}$ at concentrations ranging from 50 to 100 μM for 72 hr inhibited GSC proliferation (Gonzalez-Sanchez et al., 2016) and their stem cell phenotype (Gangoso et al., 2014).

It has been proposed that the culture of human glioblastoma explants provides a flexible and rapid platform for drug screening in a patient-specific fashion (Bayin et al., 2016). Therefore, in addition to studying the effect of TAT-Cx43$_{266-283}$ on GSC migration and invasion, we investigated its anti-tumor effect on freshly removed surgical specimens as undissociated tumor blocks. Thus, explants from

Please cite this article in press as: Jaraíz-Rodríguez et al., A Short Region of Connexin43 Reduces Human Glioma Stem Cell Migration, Invasion, and Survival through Src, PTEN, and FAK, Stem Cell Reports (2017), http://dx.doi.org/10.1016/j.stemcr.2017.06.007

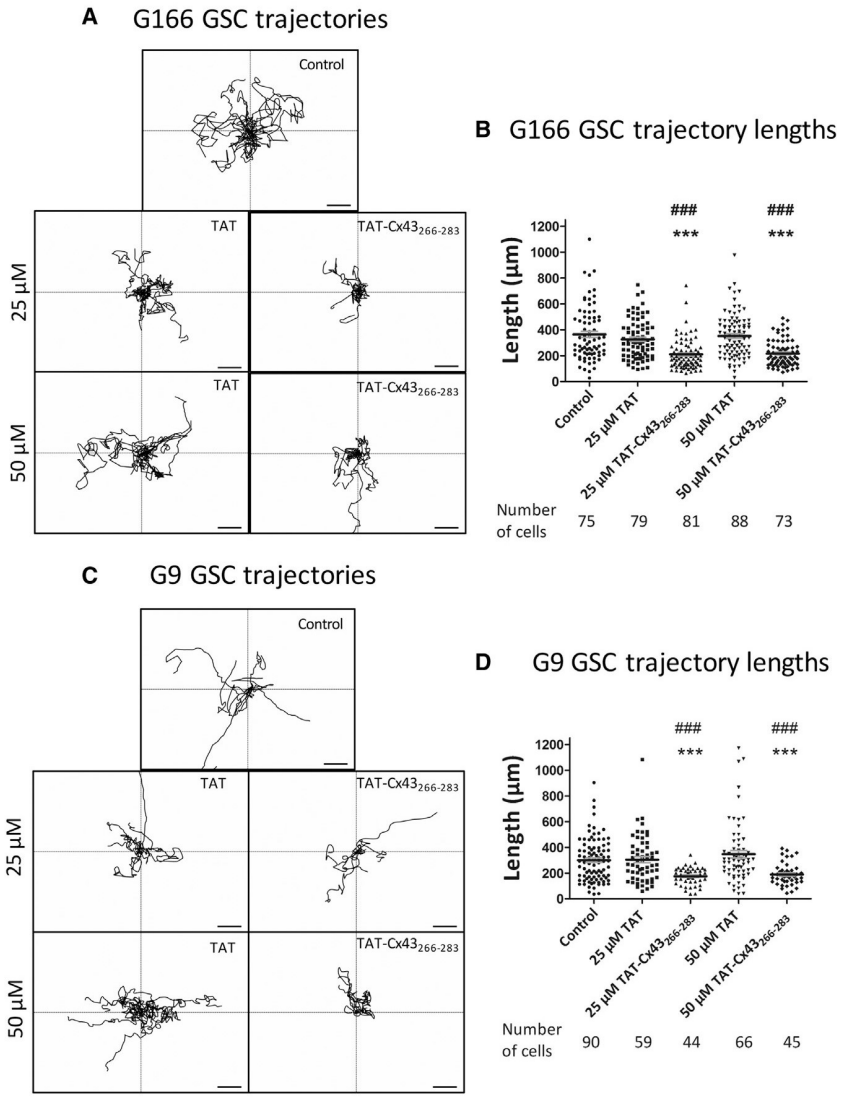

Figure 3. TAT-Cx43$_{266-283}$ Reduces GSC Motility

G166 (A and B) or primary G9 GSCs (C and D) were incubated with 25 or 50 µM TAT or TAT-Cx43$_{266-283}$, and their random movements were recorded by time-lapse microscopy for 12 hr (representative movies from primary G9 GSCs are available as Supplemental Information Movies S1, S2, and S3). Track-plots showing the trajectories described by nine representative G166 GSCs (A) or seven primary G9 GSCs (C). The origin of each cell trajectory is at the intersection of the x and y axes. Scale bars, 50 µm. (B and D) The migration length was extracted from the track-plots using the total path length described by each individual cell in at least six movies from three independent experiments. The line bisecting the plot corresponds to the mean (ANOVA; ***$p < 0.001$; TAT-Cx43$_{266-283}$ versus control, ###$p < 0.001$; TAT-Cx43$_{266-283}$ versus TAT). Non-significant differences were found when control, 25 µM TAT and 50 µM TAT levels were compared. The trajectories of cells that died during the time lapse were not considered. See also Movies S1, S2, and S3.

the same tumors used to obtain GSCs were cultured immediately after surgery, exposed to 100 µM TAT or TAT-Cx43$_{266-283}$, and cell behavior was monitored by time-lapse microscopy. Despite the different cell morphologies and features found in each tumor, in the control the cells grew rapidly and exhibited high motility and proliferation consistent with the strong aggressiveness of these tumors (Figures 6A and 6B; Movies S4, S6, and S8 for primary G9, G13, and G16 GSCs, respectively; all were treated with 100 µM TAT). Because the explants were cultured in GSC medium, which favors the growth and survival of GSCs, most of the cells expressed SOX-2 and Nestin (Figure 6C). Interestingly, the movies clearly show that 100 µM TAT-Cx43$_{266-283}$ reduced cell motility and proliferation and promoted cell death (Movies S5, S7, and S9 for G9, G13, and G16, respectively). Consequently, the change in cell number from the beginning to the end of the experiment was strongly reduced in G9, G13, or G16 explants by 100 µM TAT-Cx43$_{266-283}$ compared with treatments with 100 µM TAT or with their corresponding controls (Figures 6A and 6B; Movies S5, S7, and S9 for G9, G13, and G16, respectively).

It should be mentioned that, over the course of these experiments, we received two surgical specimens that were finally diagnosed as neuroblastoma (N6) and oligodendroglioma (O17) instead of glioblastoma. Intriguingly, 100 µM TAT-Cx43$_{266-283}$ rapidly promoted tumor cell death in the neuroblastoma and oligodendroglioma explants (data not shown), as it did in the glioblastoma explants, suggesting that the anti-tumor effect of TAT-Cx43$_{266-283}$ is not restricted to glioblastoma.

Please cite this article in press as: Jaraíz-Rodríguez et al., A Short Region of Connexin43 Reduces Human Glioma Stem Cell Migration, Invasion, and Survival through Src, PTEN, and FAK, Stem Cell Reports (2017), http://dx.doi.org/10.1016/j.stemcr.2017.06.007

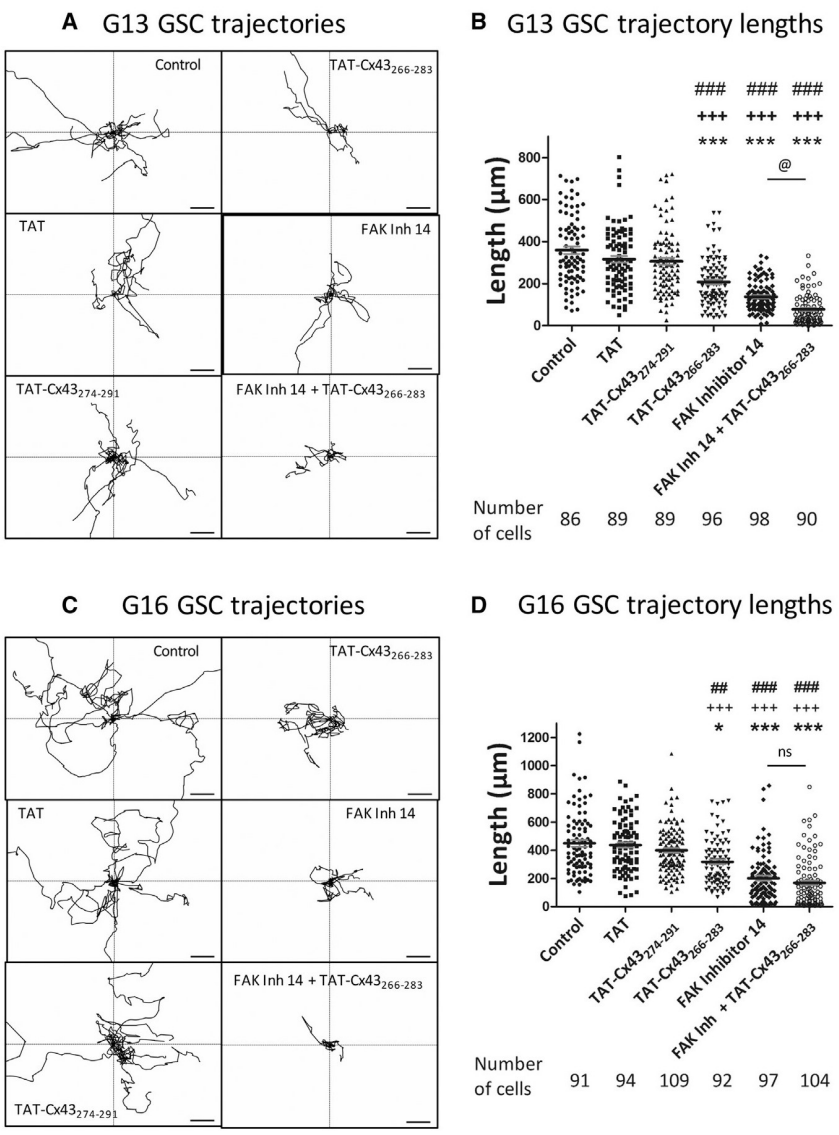

Figure 4. Specificity of the Effect of TAT-Cx43$_{266-283}$ on FAK-Dependent GSC Motility

Primary G13 (A and B) or G16 (C and D) GSCs were incubated with 50 µM TAT, TAT-Cx43$_{274-291}$, TAT-Cx43$_{266-283}$, 5 µM FAK inhibitor 14 (FAK inh 14), or 5 µM FAK inh 14 + TAT-Cx43$_{266-283}$, and their random movements were recorded by time-lapse microscopy for 14 hr. Track-plots showing the trajectories described by at least seven representative G13 (A) or G16 (C) GSCs for 14 hr. The origin of each cell's trajectory is at the intersection of the x and y axes. Scale bars, 50 µm. The migration length was extracted from the track-plots using the total path length described by each individual cell in at least ten movies from three independent experiments. The line bisecting the plot corresponds to the mean (ANOVA; ***$p < 0.001$, *$p < 0.05$; versus control; $^{+++}p < 0.001$; versus TAT; $^{###}p < 0.001$, $^{##}p < 0.01$; versus TAT-Cx43$_{274-291}$; $^{@}p < 0.05$; FAK inh 14 versus FAK inh 14 + TAT-Cx43$_{266-283}$; ns, not significant). Non-significant differences were found when the control, 50 µM TAT and 50 µM TAT-Cx43$_{274-291}$ were compared. The trajectories of cells that died during the time lapse were not considered.

DISCUSSION

Although the relationship between connexin and cancer was first described 50 years ago, the interest in this protein for use in the development of cancer therapies is increasing (Aasen et al., 2016). Our previous studies showed that restoring CX43 in glioma cells that express negligible levels of CX43 inhibits the activity of c-Src (Gangoso et al., 2014; Herrero-Gonzalez et al., 2010; Tabernero et al., 2016). This effect is caused by the recruitment of c-Src, together with its inhibitors CSK and PTEN, to a short region of CX43 from amino acids 266–283 (Gonzalez-Sanchez et al., 2016). Indeed, a cell-penetrating peptide containing this region, TAT-Cx43$_{266-283}$, is able to recruit these proteins and consequently inhibits c-Src and upregulates PTEN, mimicking the anti-proliferative effect and reversion of the stem cell phenotype promoted by CX43 in the GSC lines GliNS2 and G166 (Gangoso et al., 2014; Gonzalez-Sanchez et al., 2016). In the present study, we found that TAT-Cx43$_{266-283}$ inhibited c-Src activity and upregulated PTEN also in GSCs derived directly from patients. However, it should be considered that, although restoring CX43 in glioma cells reduces c-Src oncogenic activity, it can also have detrimental effects because of the increase in cell invasion (Naus et al., 2016). Interestingly, this study revealed that, by inhibiting c-Src and increasing PTEN, TAT-Cx43$_{266-283}$ reduced FAK activity, with subsequent inhibition in GSC migration and invasion.

Please cite this article in press as: Jaraíz-Rodríguez et al., A Short Region of Connexin43 Reduces Human Glioma Stem Cell Migration, Invasion, and Survival through Src, PTEN, and FAK, Stem Cell Reports (2017), http://dx.doi.org/10.1016/j.stemcr.2017.06.007

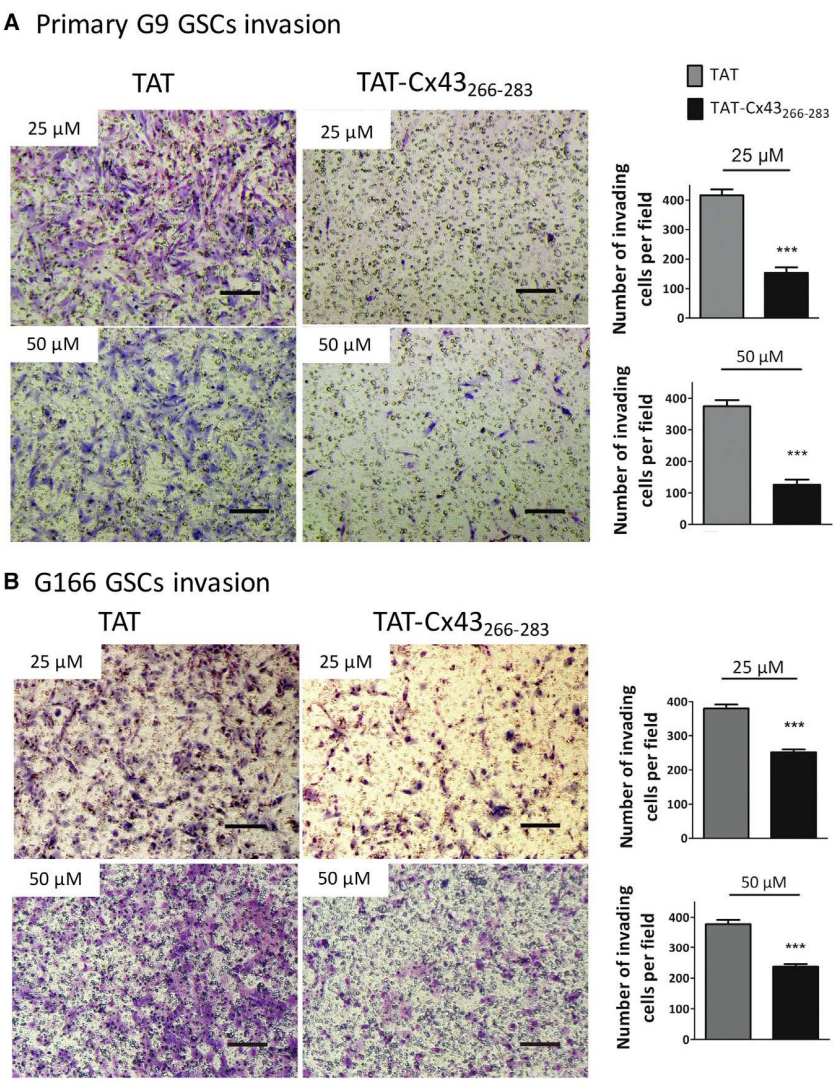

Figure 5. TAT-Cx43$_{266-283}$ Reduces GSC Invasion

Primary (A) or G166 (B) GSC invasion was analyzed using a transwell Matrigel invasion assay. Cells were incubated with TAT or TAT-Cx43$_{266-283}$ and were allowed to invade for 15 hr. The results are expressed as the number of invading cells per field ± SEM. At least five fields per insert in nine inserts from three independent experiments were counted. Scale bars, 100 μm (***$p < 0.001$; t test). See also Figures S3 and S4.

It is well known that CX43 plays a significant role in cell migration, impacting adhesion (Elias et al., 2007), cytoskeletal rearrangements, and invasiveness (reviewed in Naus et al., 2016). Thus, the C-terminal domain of CX43 interacts with crucial proteins for cell motility, such as ZO-1 (Toyofuku et al., 2001), tubulin (Saidi Brikci-Nigassa et al., 2012), debrin (Ambrosi et al., 2016), and binding partners of these proteins, such as F-actin. In addition, CX43 can increase gap junctional communication between tumor and stromal cells, causing a diffusion of molecules that contribute to tumor cell invasion or metastasis, such as microRNAs (Hong et al., 2015) or cGAMP (Chen et al., 2016). Furthermore, the C-terminal domain of CX43 can regulate signaling molecules that are involved in migration, such as p38 MAPK (Behrens et al., 2010) or c-Src (Herrero-Gonzalez et al., 2010). Therefore, it is not surprising that the resulting effect of CX43 on migration and invasion varies depending on the cellular context (Naus et al., 2016), such as the tumor microenvironment or level of activity of the partners of CX43. For instance, in glioma cells, some studies show that CX43 increases invasiveness (Lin et al., 2002; Oliveira et al., 2005; Osswald et al., 2015; Strale et al., 2012). However, others show the opposite effect: that downregulation of CX43 promotes glioma migration (Aftab et al., 2015).

To avoid this multifactorial effect, we used a short region of CX43 (from amino acids 266–283). This region lacks cytoskeleton-binding motifs and is not able to form gap junction channels; however, it retains its ability to inhibit c-Src activity (Gangoso et al., 2014; Gonzalez-Sanchez et al., 2016). As mentioned in the Introduction, c-Src is a key regulator of glioma cell migration and invasion because it phosphorylates and activates FAK (Calalb et al., 1995) and

Please cite this article in press as: Jaraíz-Rodríguez et al., A Short Region of Connexin43 Reduces Human Glioma Stem Cell Migration, Invasion, and Survival through Src, PTEN, and FAK, Stem Cell Reports (2017), http://dx.doi.org/10.1016/j.stemcr.2017.06.007

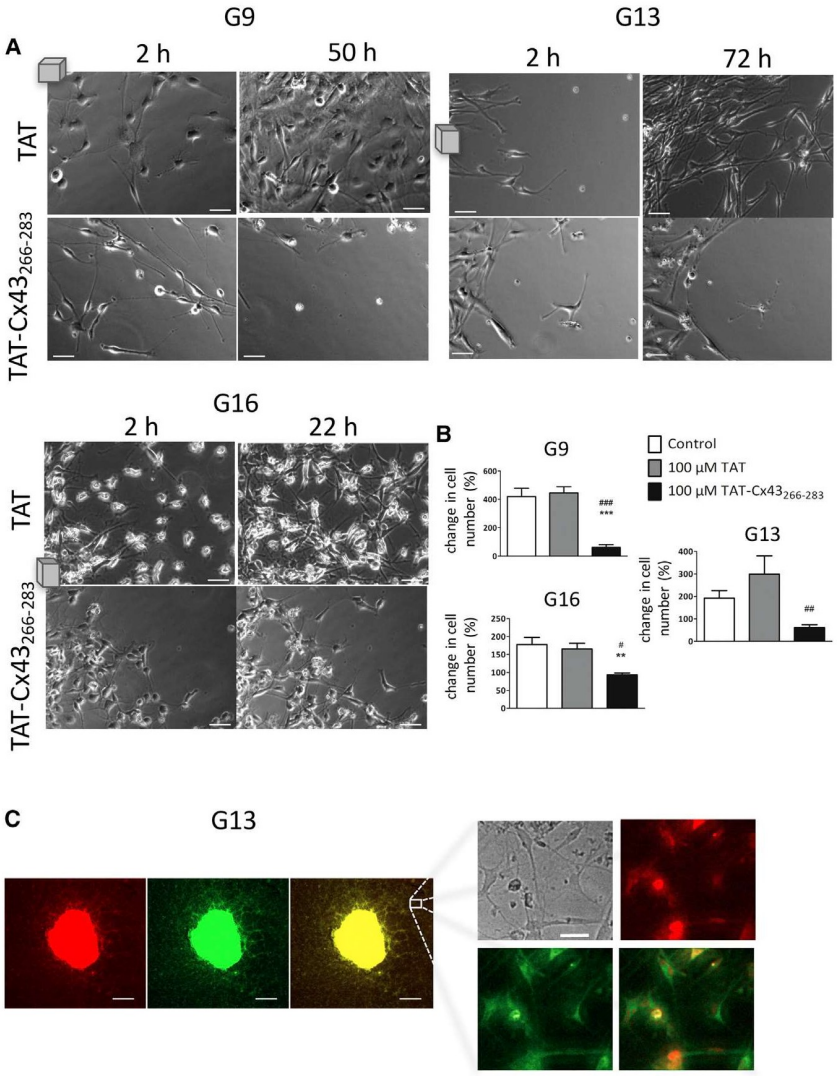

Figure 6. TAT-Cx43$_{266-283}$ Reduces Growth, Migration, and Survival in Patient-Derived Glioblastoma Explants

G9, G13, and G16 glioma explants were cultured in GSC medium and incubated in the absence (control) or presence of 100 μM TAT or TAT-Cx43$_{266-283}$ for the indicated times.

(A) Phase-contrast images of the same field showing cells growing and spreading from G9, G13, or G16 glioblastoma explants at the beginning and at the end of the experiment. Scale bars, 50 μm. Cells were recorded by time-lapse microscopy. The blocks indicate the location of the glioblastoma explants. The full movies are available as Supplemental Information Movies S4, S5, S6, S7, S8, and S9, showing the reduction in the cell growth, migration, and survival of the explants treated with TAT-Cx43$_{266-283}$.

(B) Change in cell number per field from the beginning to the end of the experiment expressed as percentage of the cells found at the beginning of the experiment. The results are the means ± SEM of three to six fields in explants from G9, G13, or G16 tumors (ANOVA; ***$p < 0.001$, **$p < 0.01$; TAT-Cx43$_{266-283}$ versus control; $^{###}p < 0.001$, $^{##}p < 0.01$, $^{#}p < 0.05$; TAT-Cx43$_{266-283}$ versus TAT).

(C) SOX-2 (red), Nestin (green) immunostaining, and merged images of the same field showing a representative explant from the G13 tumor. Scale bars, 500 μm. A magnified inset showing that most cells express these GSC markers. Scale bar, 50 μm. See also Movies S4, S5, S6, S7, S8, and S9.

promotes degradation of the tumor suppressor protein PTEN (Lu et al., 2003), whose phosphatase activity inhibits FAK (Cai et al., 2005; Tamura et al., 1998) (Figure 7A). Indeed, our results show that TAT-Cx43$_{266-283}$ inhibits c-Src activity and upregulates PTEN, with a subsequent decrease in FAK activity (Figure 7B). Src, PTEN, and FAK are crucial to trigger a cascade of events that lead to cell migration and invasion (Mitra and Schlaepfer, 2006; Yamada and Araki, 2001). Consistent with these studies, our time-lapse movies revealed that random GSC movement is reduced by the presence of TAT-Cx43$_{266-283}$, as judged by the length of the GSC trajectories. Furthermore, TAT-Cx43$_{266-283}$ strongly impaired the ability of GSCs to degrade the extracellular matrix (Matrigel) and invade transwells, consistent with a reduction in their invasive capacity.

Despite the intertumoral heterogeneity, all malignant gliomas share one conserved feature, aggressive invasiveness (Cuddapah et al., 2014), which is one of the most important consequences of the oncogenic activity of c-Src (Lund et al., 2006), specifically in GSCs (Liu et al., 2016). These cells exhibit a high level of c-Src activity (Han et al., 2014) and PTEN deficiency (Duan et al., 2015), which are required to invade the brain parenchyma, escaping surgery (Cheng et al., 2011; Garcia et al., 2010). As GSCs are resistant to conventional therapy and are highly tumorigenic, they are thought to be the main cause of recurrence after surgery and are consequently responsible for the poor survival of these patients (Chen et al., 2012; Dirks, 2010). Therefore, the results presented in this study showing inhibition of primary GSC migration

Please cite this article in press as: Jaraíz-Rodríguez et al., A Short Region of Connexin43 Reduces Human Glioma Stem Cell Migration, Invasion, and Survival through Src, PTEN, and FAK, Stem Cell Reports (2017), http://dx.doi.org/10.1016/j.stemcr.2017.06.007

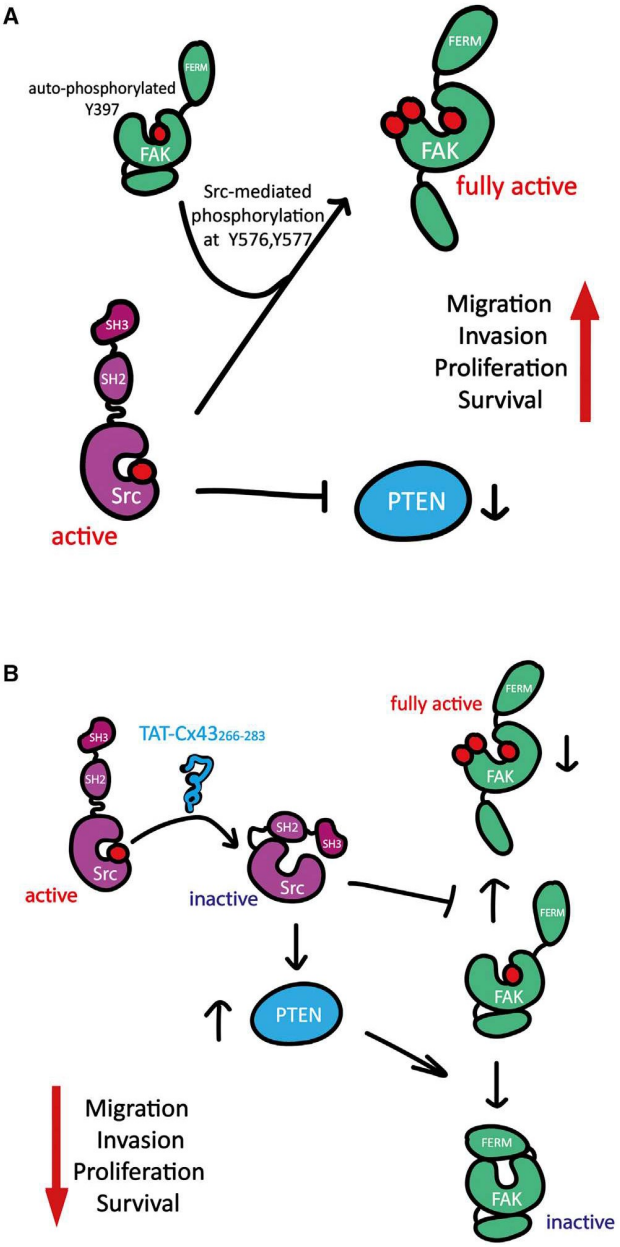

Figure 7. TAT-Cx43$_{266-283}$ Targets Src, PTEN, and FAK in GSCs

(A) In GSCs, active c-Src phosphorylates FAK at Y576 and Y577, thus fully activating FAK. Active c-Src also promotes the degradation of PTEN, an important inhibitor of FAK. The activated Src-FAK axis, together with low levels of PTEN are crucial to trigger the cascade of events leading to cell migration, invasion, proliferation, and survival. (B) TAT-Cx43$_{266-283}$ inhibits c-Src activity together with a strong upregulation of PTEN expression. As a consequence, there is a decrease in the phosphorylation of FAK at Y576 and Y577 by the low levels of active c-Src. In addition, the PTEN upregulation contributes to FAK inactivation by dephosphorylation. Altogether, these molecular changes reduce the capacity of the GSCs to migrate, invade, proliferate, and survive.

and invasion promoted by TAT-Cx43$_{266-283}$ are very promising for therapeutic development against this incurable disease.

Notably, TAT-Cx43$_{266-283}$ targets Src and PTEN, which are critical nodes in signaling pathways that impact proliferation, migration, invasion, and survival (Knobbe et al., 2002; Zhang et al., 2011). Furthermore, *PTEN* is one of the most frequent genetic alterations found in glioblastomas (Cancer Genome Atlas Research Network, 2008) and, although genetic analyses did not show any *SRC* alterations in glioblastoma, tyrosine kinase phosphorylation assays have shown that Src activation is a common event in glioblastoma (Du et al., 2009). Therefore, it is not unexpected that TAT-Cx43$_{266-283}$ exerted a potent anti-tumor effect on most of the glioblastoma patient explants analyzed in this study (Movies S4, S5, S6, S7, S8, and S9). In fact, these results should be highlighted because of the accuracy of patient-derived models in the identification of effective cancer treatments (Bayin et al., 2016; Crystal et al., 2014).

In conclusion, a region of CX43 (amino acids 266–283), by targeting c-Src, PTEN, and FAK, exerts a potent anti-tumor effect in patient-derived glioblastoma cells, which includes an impairment of GSC migration and invasion. This study reinforces the relevance of this sequence and encourages further research for the development of new therapies against glioblastoma.

EXPERIMENTAL PROCEDURES

Ethics Statement

Patients provided written informed consent to participate in the study, and tumor samples and cell culture brain tumor samples were obtained following local ethical board approval at the Service of Neurosurgery in the Hospital Universitario de Salamanca (Spain). The study was approved by the bioethics committee of the University of Salamanca and Junta de Castilla y León (Spain).

GSC Cultures

G166 GSCs were obtained from BioRep (Milan, Italy) (Pollard et al., 2009). Primary GSCs were obtained and cultured as described previously (Thirant et al., 2011). In brief, immediately after surgery, the tumor samples (G9, G12, G13, G15, and G16, diagnosed as classic glioblastomas; N6, a neuroblastoma; and O17, an oligodendroglioma) were washed and deprived of vessels in PBS. After mechanical dissociation, the samples were subjected to enzymatic dissociation with Accutase (Sigma-Aldrich Química, Madrid, Spain) for 15–20 min at 37°C. These solutions were then filtered and centrifuged at 1,000 × *g* for 5 min. The G166 and primary GSCs were cultured in RHB-A medium (Takara Bio, Condalab, Madrid, Spain) supplemented with 2% B27 (Life Technologies, Thermo Fisher Scientific, Waltham, USA), 1% N2 supplement (Life Technologies), 20 ng/mL epidermal growth factor (EGF), and 20 ng/mL basic fibroblast growth factor (b-FGF) (PeproTech,

Please cite this article in press as: Jaraíz-Rodríguez et al., A Short Region of Connexin43 Reduces Human Glioma Stem Cell Migration, Invasion, and Survival through Src, PTEN, and FAK, Stem Cell Reports (2017), http://dx.doi.org/10.1016/j.stemcr.2017.06.007

London, UK) under adherent conditions as described by Pollard et al. (2009). Culture plates were coated with 10 μg/mL laminin (Life Technologies) for 2 hr before use. The cells were maintained at 37°C in an atmosphere of 95% air/5% CO_2 and with 90%–95% humidity. The G166 and primary GSCs were grown to confluency, dissociated using Accutase, and then split. We routinely used cultures expanded for no more than 15 passages.

Cell Treatments

The synthetic peptides (>85% pure) were obtained from GenScript (Piscataway, NJ, USA). YGRKKRRQRRR was used as the TAT sequence, which is responsible for the cell penetration of the peptides (Gangoso et al., 2014). The TAT-$Cx43_{266-283}$ sequence was TAT-AYFNGCSSPTAPLSPMSP and the TAT-$Cx43_{274-291}$ sequence was TAT-PTAPLSPMSPGYKLVTG. The peptides were used at different concentrations (25, 50, or 100 μM) in culture medium at 37°C for the indicated time. FAK inhibitor 14 (SML0837) was obtained from Sigma and used at 5 μM.

Immunocytochemistry

Cells were fixed in 4% paraformaldehyde for 20 min. A mouse monoclonal antibody against human Nestin (1:200; Abcam, Cambridge, UK; Ref. ab18102) was applied overnight at 4°C, followed by incubation with an Alexa Fluor 488-conjugated anti-mouse immunoglobulin G (IgG) antibody (1:1,000; Life Technologies; Ref. A-11029) for 2 hr. A rabbit polyclonal antibody against SOX-2 (1:200; Abcam; Ref. ab97959) was applied overnight at 4°C, followed by incubation with an Alexa Fluor 594-conjugated anti-rabbit IgG antibody (1:1,000; Life Technologies; Ref. A-11012) for 2 hr. The cells were then mounted using a SlowFade Light Antifade Kit (Life Technologies), and they were analyzed on a Leica inverted fluorescence microscope connected to a digital video camera (Leica DC 100; Leica Microsystems, Wetzlar, Germany).

Migration Assays

G166 or primary GSCs were plated at a low density (5,000 cells/cm^2) in 24-well plates. Once the cells were attached, TAT or TAT-$Cx43_{266-283}$ was added at 25 or 50 μM, and the cells were allowed to equilibrate for 1–3 hr in the microscope incubator before imaging. Random cell movement was recorded by time-lapse live-cell imaging for 12–14 hr. The total duration of the treatment was always 15 hr. Every 10 min, phase-contrast photographs of each experimental condition were taken with an inverted Zeiss Axio Observer Z1 microscope for live-cell imaging (Carl Zeiss Microscopy, LLC, USA) coupled to an AxioCam MRm camera. The system included an automated XY stage controller and a humidified incubator set at 37°C and 5% CO_2. Image stacks were processed, and cell movement was manually tracked and further analyzed using Zen imaging software (Carl Zeiss Microscopy). Average cell length was calculated in at least six independent movies from three independent experiments.

Glioblastoma Explant Cultures

The tumor samples, immediately after surgery, were washed, deprived of vessels in PBS and finely minced into approximately 1-mm^3 pieces. The explants were plated individually in 24-well plates and cultured in RHB-A medium (Takara Bio, Condalab, Madrid, Spain) supplemented with 2% B27 (Life Technologies, Thermo Fisher Scientific, Waltham, USA), 1% N2 supplement (Life Technologies), 20 ng/mL EGF, and 20 ng/mL b-FGF (PeproTech, London, UK), as described previously (Bayin et al., 2016). Culture plates were coated with 10 μg/mL laminin (Life Technologies) for 2 hr before use. The tumor blocks were maintained at 37°C in an atmosphere of 95% air/5% CO_2 and with 90%–95% humidity. Once the explants were attached (after 24–72 hr), TAT or TAT-$Cx43_{266-283}$ was added at 100 μM, and the cells were allowed to equilibrate for 1–3 hr in the microscope incubator before imaging. The cells were recorded by time-lapse live-cell imaging for the indicated times. Every 10 min, phase-contrast photographs of each experimental condition were taken with an inverted Zeiss Axio Observer Z1 microscope for live-cell imaging (Carl Zeiss Microscopy, LLC, USA) coupled to an AxioCam MRm camera. The system included an automated XY stage controller and a humidified incubator set at 37°C and 5% CO_2. Image stacks were processed using Zen imaging software (Carl Zeiss Microscopy).

Invasion Assays

Cell invasion was measured in Matrigel (Corning, Amsterdam, The Netherlands)-coated transwell inserts (Merck Millipore, Madrid, Spain) containing polyethylene terephthalate filters with 8-μm pores. The inserts were coated with 100 μL of 1 mg/mL Matrigel matrix according to the manufacturer's recommendations. Next, 7.5×10^4 cells in 200 μL of serum-free medium were plated in the upper chamber, whereas 500 μL of medium supplemented with 10% fetal bovine serum (Gibco, Life Technologies) was added to the lower well. The indicated treatments were added, and the cells were allowed to invade for 15 hr. Non-invading cells were carefully removed with wet cotton swabs from the top of the membranes. The invading cells of the lower surface were fixed with 4% paraformaldehyde for 10 min, washed with PBS, and stained with Giemsa for 10 min. The inserts were washed with PBS and allowed to dry. The invading cells were counted in at least five random fields per insert from three independent experiments. Images were taken using a Leica microscope connected to a digital camera (Leica DFC500).

Western Blot Analysis

Western blotting was performed as described previously (Herrero-Gonzalez et al., 2010). In brief, equivalent amounts of proteins (20 μg per lane) were separated on NuPAGE Novex Bis-Tris (4%–12%) midi gels (Life Technologies). The proteins were transblotted using an iBlot dry blotting system (Life Technologies). After blocking, the membranes were incubated overnight at 4°C with the primary antibodies against Y416 Src (1:200; Cell Signaling, Danvers, MA, USA; Ref. 2101), total Src (1:500; Cell Signaling; Ref. 2108), PTEN (1:500; Cell Signaling; Ref. 9556S), Y397 FAK (1:1,000; Life Technologies; Ref. 44-624G), Y576 FAK (1:500; Life Technologies; Ref. 44652G), Y577 FAK (1:500; Life Technologies; Ref. 44-614G), and total FAK (1:500; Life Technologies; Ref. AHO0502). The antibodies against glyceraldehyde phosphate dehydrogenase (GAPDH, 1:15,000; Ambion, Thermo Fisher Scientific; Ref. AM4300) or alpha-actinin (1:1,000; Chemicon International, Merck Millipore; Ref. MAB1682) were used as a loading control. After extensive washing, the membranes were incubated

Please cite this article in press as: Jaraíz-Rodríguez et al., A Short Region of Connexin43 Reduces Human Glioma Stem Cell Migration, Invasion, and Survival through Src, PTEN, and FAK, Stem Cell Reports (2017), http://dx.doi.org/10.1016/j.stemcr.2017.06.007

with peroxidase-conjugated anti-rabbit IgG or the anti-mouse IgG antibody (Santa Cruz Biotechnology, Dallas, TX, USA; Refs. sc-2030 and sc-2005) in TTBS and developed with a chemiluminescent substrate (Western Blotting Luminol Reagent; Santa Cruz Biotechnology). X-ray films were obtained from Fujifilm (Madrid, Spain).

MTT Assay

Cells cultured at 37°C in 24-well plates were incubated in the dark for 75 min with 300 μL of RHB-A medium containing 0.5 mg/mL MTT (Sigma). The medium was then removed, and the cells were incubated for 10 min in the dark with DMSO (500 μL per well) with mild shaking. Finally, the absorbance was measured at a wavelength of 570 nm using a microplate reader (Appliskan 2001; Thermo Electron Corporation, Thermo Scientific, Madrid, Spain).

Statistical Analysis

The results are expressed as the mean ± SEM of at least three independent experiments. Statistical analyses were carried out using Student's t test when two groups were compared. For the comparison of more than two groups, an ANOVA (one-way ANOVA) was used, followed by the appropriate post-test (Tukey). Values were considered significant when $p < 0.05$.

SUPPLEMENTAL INFORMATION

Supplemental Information includes four figures and nine movies and can be found with this article online at http://dx.doi.org/10.1016/j.stemcr.2017.06.007.

AUTHOR CONTRIBUTIONS

M.J.-R., contributed to the experimental design and development, data acquisition, analysis, and interpretation, drafting and revision of the article for important intellectual content, and approved the final version for publication. M.D.T., design and custody of patients' written informed consent, design and processing of ethical board approval at the Service of Neurosurgery in the Hospital Universitario de Salamanca (Spain), transfer of patient-derived samples, revision of the article for important intellectual content, and approved the final version for publication. M.G.-T., design and processing for ethical board approval at the Service of Neurosurgery in the Hospital Universitario de Salamanca (Spain), transfer of patient-derived samples, revision of the article for important intellectual content, and approved the final version for publication. A. Otero, glioblastoma surgery, diagnosis, obtained written informed consent from patients, revised the article for important intellectual content, and approved the final version for publication. A. Orfao, design of patients' written informed consent, design and processing for approval from the ethical board at the Service of Neurosurgery in the Hospital Universitario de Salamanca (Spain), revision of the article for important intellectual content, and approved the final version for publication. J.M.M., contributed to the experimental design and data interpretation, revised the article for important intellectual content, and approved the final version for publication. A.T., conceived and designed the experiments, designed and processed documentation for bioethics committee approval from the University of Salamanca and Junta de Castilla y León (Spain), supervised the experimental development and analysis, interpreted the data, drafted the article, and approved the final version for publication.

ACKNOWLEDGMENTS

We thank Daniel Lietha for helping with the FAK pathway analysis and H. Chneiweiss for his help with the primary GSC culture protocols. We are grateful for the technical assistance of T. del Rey. This work was supported by the Ministerio de Economía y Competitividad, Spain (FEDER BFU2015-70040-R), Junta de Castilla y León, Spain (FEDER SA026U16), and Fundación Ramón Areces. M.J.-R. was a fellowship recipient from the Junta de Castilla y León and the European Social Fund.

Received: January 25, 2017
Revised: June 13, 2017
Accepted: June 14, 2017
Published: July 13, 2017

REFERENCES

Aasen, T., Mesnil, M., Naus, C.C., Lampe, P.D., and Laird, D.W. (2016). Gap junctions and cancer: communicating for 50 years. Nat. Rev. Cancer *16*, 775–788.

Aftab, Q., Sin, W.C., and Naus, C.C. (2015). Reduction in gap junction intercellular communication promotes glioma migration. Oncotarget *6*, 11447–11464.

Ambrosi, C., Ren, C., Spagnol, G., Cavin, G., Cone, A., Grintsevich, E.E., Sosinsky, G.E., and Sorgen, P.L. (2016). Connexin43 forms supramolecular complexes through non-overlapping binding sites for drebrin, tubulin, and ZO-1. PLoS One *11*, e0157073.

Bayin, N.S., Ma, L., Thomas, C., Baitalmal, R., Sure, A., Fansiwala, K., Bustoros, M., Golfinos, J.G., Pacione, D., Snuderl, M., et al. (2016). Patient-specific screening using high-grade glioma explants to determine potential radiosensitization by a TGF-beta small molecule inhibitor. Neoplasia *18*, 795–805.

Behrens, J., Kameritsch, P., Wallner, S., Pohl, U., and Pogoda, K. (2010). The carboxyl tail of Cx43 augments p38 mediated cell migration in a gap junction-independent manner. Eur. J. Cell Biol. *89*, 828–838.

Cai, X.M., Tao, B.B., Wang, L.Y., Liang, Y.L., Jin, J.W., Yang, Y., Hu, Y.L., and Zha, X.L. (2005). Protein phosphatase activity of PTEN inhibited the invasion of glioma cells with epidermal growth factor receptor mutation type III expression. Int. J. Cancer *117*, 905–912.

Calalb, M.B., Polte, T.R., and Hanks, S.K. (1995). Tyrosine phosphorylation of focal adhesion kinase at sites in the catalytic domain regulates kinase activity: a role for Src family kinases. Mol. Cell Biol. *15*, 954–963.

Carragher, N.O., Walker, S.M., Scott Carragher, L.A., Harris, F., Sawyer, T.K., Brunton, V.G., Ozanne, B.W., and Frame, M.C. (2006). Calpain 2 and Src dependence distinguishes mesenchymal and amoeboid modes of tumour cell invasion: a link to integrin function. Oncogene *25*, 5726–5740.

Cancer Genome Atlas Research Network. (2008). Comprehensive genomic characterization defines human glioblastoma genes and core pathways. Nature *455*, 1061–1068.

Chen, J., Li, Y., Yu, T.S., McKay, R.M., Burns, D.K., Kernie, S.G., and Parada, L.F. (2012). A restricted cell population propagates glioblastoma growth after chemotherapy. Nature *488*, 522–526.

Chen, Q., Boire, A., Jin, X., Valiente, M., Er, E.E., Lopez-Soto, A., Jacob, L.S., Patwa, R., Shah, H., Xu, K., et al. (2016). Carcinoma-astrocyte gap junctions promote brain metastasis by cGAMP transfer. Nature *533*, 493–498.

Cheng, L., Wu, Q., Guryanova, O.A., Huang, Z., Huang, Q., Rich, J.N., and Bao, S. (2011). Elevated invasive potential of glioblastoma stem cells. Biochem. Biophys. Res. Commun. *406*, 643–648.

Crespin, S., Fromont, G., Wager, M., Levillain, P., Cronier, L., Monvoisin, A., Defamie, N., and Mesnil, M. (2016). Expression of a gap junction protein, connexin43, in a large panel of human gliomas: new insights. Cancer Med. *5*, 1742–1752.

Crystal, A.S., Shaw, A.T., Sequist, L.V., Friboulet, L., Niederst, M.J., Lockerman, E.L., Frias, R.L., Gainor, J.F., Amzallag, A., Greninger, P., et al. (2014). Patient-derived models of acquired resistance can identify effective drug combinations for cancer. Science *346*, 1480–1486.

Cuddapah, V.A., Robel, S., Watkins, S., and Sontheimer, H. (2014). A neurocentric perspective on glioma invasion. Nat. Rev. Neurosci. *15*, 455–465.

Dirks, P.B. (2010). Brain tumor stem cells: the cancer stem cell hypothesis writ large. Mol. Oncol. *4*, 420–430.

Du, J., Bernasconi, P., Clauser, K.R., Mani, D.R., Finn, S.P., Beroukhim, R., Burns, M., Julian, B., Peng, X.P., Hieronymus, H., et al. (2009). Bead-based profiling of tyrosine kinase phosphorylation identifies SRC as a potential target for glioblastoma therapy. Nat. Biotechnol. *27*, 77–83.

Duan, S., Yuan, G., Liu, X., Ren, R., Li, J., Zhang, W., Wu, J., Xu, X., Fu, L., Li, Y., et al. (2015). PTEN deficiency reprogrammes human neural stem cells towards a glioblastoma stem cell-like phenotype. Nat. Commun. *6*, 10068.

Elias, L.A., Wang, D.D., and Kriegstein, A.R. (2007). Gap junction adhesion is necessary for radial migration in the neocortex. Nature *448*, 901–907.

Frolov, A., Evans, I.M., Li, N., Sidlauskas, K., Paliashvili, K., Lockwood, N., Barrett, A., Brandner, S., Zachary, I.C., and Frankel, P. (2016). Imatinib and Nilotinib increase glioblastoma cell invasion via Abl-independent stimulation of p130Cas and FAK signalling. Sci. Rep. *6*, 27378.

Gangoso, E., Thirant, C., Chneiweiss, H., Medina, J.M., and Tabernero, A. (2014). A cell-penetrating peptide based on the interaction between c-Src and connexin43 reverses glioma stem cell phenotype. Cell Death Dis. *5*, e1023.

Garcia, J.L., Perez-Caro, M., Gomez-Moreta, J.A., Gonzalez, F., Ortiz, J., Blanco, O., Sancho, M., Hernandez-Rivas, J.M., Gonzalez-Sarmiento, R., and Sanchez-Martin, M. (2010). Molecular analysis of ex-vivo CD133+ GBM cells revealed a common invasive and angiogenic profile but different proliferative signatures among high grade gliomas. BMC Cancer *10*, 454.

Giaume, C., Koulakoff, A., Roux, L., Holcman, D., and Rouach, N. (2010). Astroglial networks: a step further in neuroglial and gliovascular interactions. Nat. Rev. Neurosci. *11*, 87–99.

Gilbert, M.R., Dignam, J.J., Armstrong, T.S., Wefel, J.S., Blumenthal, D.T., Vogelbaum, M.A., Colman, H., Chakravarti, A., Pugh, S., Won, M., et al. (2014). A randomized trial of bevacizumab for newly diagnosed glioblastoma. N. Engl. J. Med. *370*, 699–708.

Gonzalez-Sanchez, A., Jaraiz-Rodriguez, M., Dominguez-Prieto, M., Herrero-Gonzalez, S., Medina, J.M., and Tabernero, A. (2016). Connexin43 recruits PTEN and Csk to inhibit c-Src activity in glioma cells and astrocytes. Oncotarget *7*, 49819–49833.

Han, X., Zhang, W., Yang, X., Wheeler, C.G., Langford, C.P., Wu, L., Filippova, N., Friedman, G.K., Ding, Q., Fathallah-Shaykh, H.M., et al. (2014). The role of Src family kinases in growth and migration of glioma stem cells. Int. J. Oncol. *45*, 302–310.

Herrero-Gonzalez, S., Gangoso, E., Giaume, C., Naus, C.C., Medina, J.M., and Tabernero, A. (2010). Connexin43 inhibits the oncogenic activity of c-Src in C6 glioma cells. Oncogene *29*, 5712–5723.

Hong, X., Sin, W.C., Harris, A.L., and Naus, C.C. (2015). Gap junctions modulate glioma invasion by direct transfer of microRNA. Oncotarget *6*, 15566–15577.

Huang, R.-P., Hossain, M., Sehgal, A., and Boynton, A. (1999). Reduced connexin43 expression in high-grade human brain glioma cells. J. Surg. Oncol. *70*, 21–24.

Hughes, C.S., Postovit, L.M., and Lajoie, G.A. (2010). Matrigel: a complex protein mixture required for optimal growth of cell culture. Proteomics *10*, 1886–1890.

Ilić, D., Furuta, Y., Kanazawa, S., Takeda, N., Sobue, K., Nakatsuji, N., Nomura, S., Fujimoto, J., Okada, M., and Yamamoto, T. (1995). Reduced cell motility and enhanced focal adhesion contact formation in cells from FAK-deficient mice. Nature *377*, 539–544.

Klinghoffer, R.A., Sachsenmaier, C., Cooper, J.A., and Soriano, P. (1999). Src family kinases are required for integrin but not PDGFR signal transduction. EMBO J. *18*, 2459–2471.

Kmiecik, T.E., and Shalloway, D. (1987). Activation and suppression of pp60c-src transforming ability by mutation of its primary sites of tyrosine phosphorylation. Cell *49*, 65–73.

Knobbe, C.B., Merlo, A., and Reifenberger, G. (2002). Pten signaling in gliomas. Neuro Oncol. *4*, 196–211.

Lin, J.H., Takano, T., Cotrina, M.L., Arcuino, G., Kang, J., Liu, S., Gao, Q., Jiang, L., Li, F., Lichtenberg-Frate, H., et al. (2002). Connexin 43 enhances the adhesivity and mediates the invasion of malignant glioma cells. J. Neurosci. *22*, 4302–4311.

Lindemann, C., Hackmann, O., Delic, S., Schmidt, N., Reifenberger, G., and Riemenschneider, M.J. (2011). SOCS3 promoter methylation is mutually exclusive to EGFR amplification in gliomas and promotes glioma cell invasion through STAT3 and FAK activation. Acta Neuropathol. *122*, 241–251.

Liu, C., Li, Y., Xing, Y., Cao, B., Yang, F., Yang, T., Ai, Z., Wei, Y., and Jiang, J. (2016). The interaction between cancer stem cell marker CD133 and Src protein promotes focal adhesion kinase (FAK) phosphorylation and cell migration. J. Biol. Chem. *291*, 15540–15550.

Lu, Y., Yu, Q., Liu, J.H., Zhang, J., Wang, H., Koul, D., McMurray, J.S., Fang, X., Yung, W.K., Siminovitch, K.A., et al. (2003). Src family protein-tyrosine kinases alter the function of PTEN to regulate phosphatidylinositol 3-kinase/AKT cascades. J. Biol. Chem. *278*, 40057–40066.

Please cite this article in press as: Jaraíz-Rodríguez et al., A Short Region of Connexin43 Reduces Human Glioma Stem Cell Migration, Invasion, and Survival through Src, PTEN, and FAK, Stem Cell Reports (2017), http://dx.doi.org/10.1016/j.stemcr.2017.06.007

Lund, C.V., Nguyen, M.T., Owens, G.C., Pakchoian, A.J., Shaterian, A., Kruse, C.A., and Eliceiri, B.P. (2006). Reduced glioma infiltration in Src-deficient mice. J. Neurooncol. *78*, 19–29.

McLean, G.W., Carragher, N.O., Avizienyte, E., Evans, J., Brunton, V.G., and Frame, M.C. (2005). The role of focal-adhesion kinase in cancer – a new therapeutic opportunity. Nat. Rev. Cancer *5*, 505–515.

Mitra, S.K., and Schlaepfer, D.D. (2006). Integrin-regulated FAK-Src signaling in normal and cancer cells. Curr. Opin. Cell Biol. *18*, 516–523.

Naus, C.C., Aftab, Q., and Sin, W.C. (2016). Common mechanisms linking connexin43 to neural progenitor cell migration and glioma invasion. Semin. Cell Dev. Biol. *50*, 59–66.

Oliveira, R., Christov, C., Guillamo, J.S., de Bouard, S., Palfi, S., Venance, L., Tardy, M., and Peschanski, M. (2005). Contribution of gap junctional communication between tumor cells and astroglia to the invasion of the brain parenchyma by human glioblastomas. BMC Cell Biol. *6*, 7.

Osswald, M., Jung, E., Sahm, F., Solecki, G., Venkataramani, V., Blaes, J., Weil, S., Horstmann, H., Wiestler, B., Syed, M., et al. (2015). Brain tumour cells interconnect to a functional and resistant network. Nature *528*, 93–98.

Park, M.J., Kim, M.S., Park, I.C., Kang, H.S., Yoo, H., Park, S.H., Rhee, C.H., Hong, S.I., and Lee, S.H. (2002). PTEN suppresses hyaluronic acid-induced matrix metalloproteinase-9 expression in U87MG glioblastoma cells through focal adhesion kinase dephosphorylation. Cancer Res. *62*, 6318–6322.

Pollard, S.M., Yoshikawa, K., Clarke, I.D., Danovi, D., Stricker, S., Russell, R., Bayani, J., Head, R., Lee, M., Bernstein, M., et al. (2009). Glioma stem cell lines expanded in adherent culture have tumor-specific phenotypes and are suitable for chemical and genetic screens. Cell Stem Cell *4*, 568–580.

Pu, P., Xia, Z., Yu, S., and Huang, Q. (2004). Altered expression of Cx43 in astrocytic tumors. Clin. Neurol. Neurosurg. *107*, 49–54.

Riemenschneider, M.J., Mueller, W., Betensky, R.A., Mohapatra, G., and Louis, D.N. (2005). In situ analysis of integrin and growth factor receptor signaling pathways in human glioblastomas suggests overlapping relationships with focal adhesion kinase activation. Am. J. Pathol. *167*, 1379–1387.

Ruest, P.J., Roy, S., Shi, E., Mernaugh, R.L., and Hanks, S.K. (2000). Phosphospecific antibodies reveal focal adhesion kinase activation loop phosphorylation in nascent and mature focal adhesions and requirement for the autophosphorylation site. Cell Growth Differ. *11*, 41–48.

Saidi Brikci-Nigassa, A., Clement, M.J., Ha-Duong, T., Adjadj, E., Ziani, L., Pastre, D., Curmi, P.A., and Savarin, P. (2012). Phosphorylation controls the interaction of the connexin43 C-terminal domain with tubulin and microtubules. Biochemistry *51*, 4331–4342.

Shinoura, N., Chen, L., Wani, M.A., Kim, Y.G., Larson, J.J., Warnick, R.E., Simon, M., Menon, A.G., Bi, W.L., and Stambrook, P.J. (1996). Protein and messenger RNA expression of connexin43 in astrocytomas: implications in brain tumor gene therapy. J. Neurosurg. *84*, 839–845.

Soroceanu, L., Manning, T., and Sontheimer, H. (2001). Reduced expression of connexin-43 and functional gap junction coupling in human gliomas. Glia *33*, 107–117.

Strale, P.O., Clarhaut, J., Lamiche, C., Cronier, L., Mesnil, M., and Defamie, N. (2012). Down-regulation of Connexin43 expression reveals the involvement of caveolin-1 containing lipid rafts in human U251 glioblastoma cell invasion. Mol. Carcinog. *51*, 845–860.

Tabernero, A., Gangoso, E., Jaraíz-Rodríguez, M., and Medina, J.M. (2016). The role of connexin43-Src interaction in astrocytomas: a molecular puzzle. Neuroscience *323*, 183–194.

Tamura, M., Gu, J., Matsumoto, K., Aota, S., Parsons, R., and Yamada, K.M. (1998). Inhibition of cell migration, spreading, and focal adhesions by tumor suppressor PTEN. Science *280*, 1614–1617.

Thirant, C., Bessette, B., Varlet, P., Puget, S., Cadusseau, J., Tavares Sdos, R., Studler, J.M., Silvestre, D.C., Susini, A., Villa, C., et al. (2011). Clinical relevance of tumor cells with stem-like properties in pediatric brain tumors. PLoS One *6*, e16375.

Toyofuku, T., Akamatsu, Y., Zhang, H., Kuzuya, T., Tada, M., and Hori, M. (2001). c-Src regulates the interaction between connexin-43 and ZO-1 in cardiac myocytes. J. Biol. Chem. *276*, 1780–1788.

van Nimwegen, M.J., Verkoeijen, S., van Buren, L., Burg, D., and van de Water, B. (2005). Requirement for focal adhesion kinase in the early phase of mammary adenocarcinoma lung metastasis formation. Cancer Res. *65*, 4698–4706.

Yamada, K.M., and Araki, M. (2001). Tumor suppressor PTEN: modulator of cell signaling, growth, migration and apoptosis. J. Cell Sci. *114*, 2375–2382.

Yu, S.C., Xiao, H.L., Jiang, X.F., Wang, Q.L., Li, Y., Yang, X.J., Ping, Y.F., Duan, J.J., Jiang, J.Y., Ye, X.Z., et al. (2012). Connexin 43 reverses malignant phenotypes of glioma stem cells by modulating E-cadherin. Stem Cells *30*, 108–120.

Zhang, S., Huang, W.C., Li, P., Guo, H., Poh, S.B., Brady, S.W., Xiong, Y., Tseng, L.M., Li, S.H., Ding, Z., et al. (2011). Combating trastuzumab resistance by targeting SRC, a common node downstream of multiple resistance pathways. Nat. Med. *17*, 461–469.

Stem Cell Reports, Volume *9*

Supplemental Information

A Short Region of Connexin43 Reduces Human Glioma Stem Cell Migration, Invasion, and Survival through Src, PTEN, and FAK

Myriam Jaraíz-Rodríguez, Ma Dolores Tabernero, María González-Tablas, Alvaro Otero, Alberto Orfao, Jose M. Medina, and Arantxa Tabernero

Supplemental Figures and legends

Figure S1

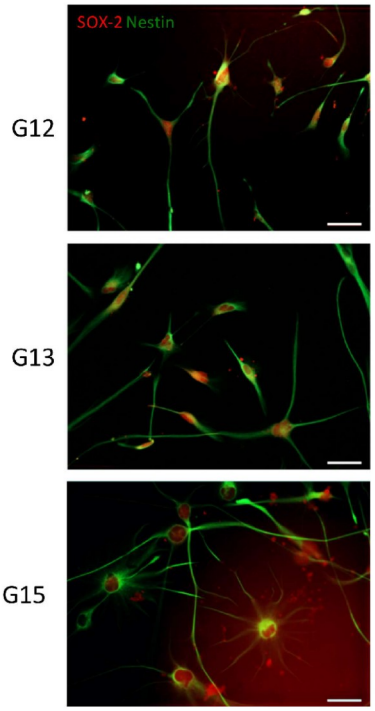

Figure S1. SOX-2 and Nestin immunostaining in primary G12, G13, and G15 GSCs. Related to Figure 1.

SOX-2 (red) and Nestin (green) merged immunostaining showing that primary G12, G13, and G15 GSCs, obtained as described in the Experimental procedures section, express these GSC markers. Bar = 50 μm.

Figure S2

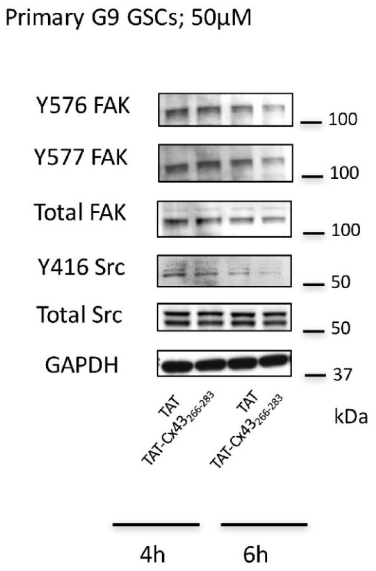

Figure S2. **Effect of TAT-Cx43$_{266-283}$ on c-Src and FAK activity in primary GSC and G166 GSC after 4 and 6h. Related to Figure 2.**

Primary G9 GSCs were incubated with 50 µM TAT or 50 µM TAT-Cx43$_{266-283}$. After 4 and 6 h, the total c-Src, Y416 c-Src, total FAK, Y576 FAK and Y577 FAK levels were analyzed by Western blotting. GAPDH was used as a loading control.

Figure S3

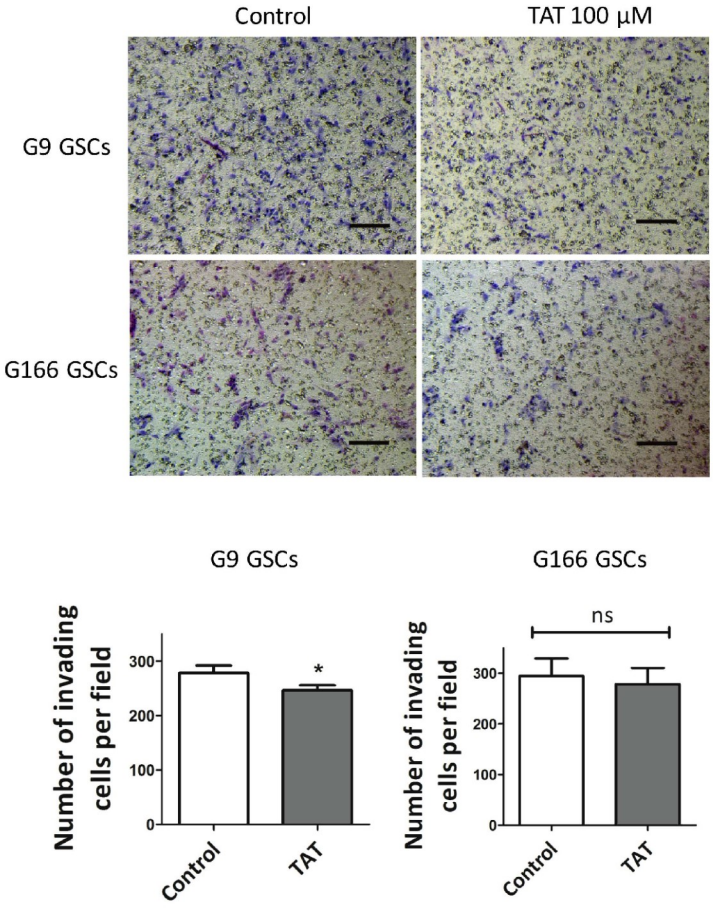

Figure S3. Effect of TAT on primary G9 GSC and G166 GSC invasion. Related to Figure 5.

Representative photomicrographs and the quantification of invading cells from the analysis of the transwell Matrigel invasion assay as described in the Experimental procedures section. Control or 100 µM TAT-treated G9 GSCs or G166 GSCs were allowed to invade for 15 h. The results are expressed as the number of invading cells per field ± s.e.m. At least five fields per insert in nine inserts from three independent experiments were counted. Bar = 100 µm. (*p<0.05; ns, not significant; TAT vs control, t-test).

Figure S4

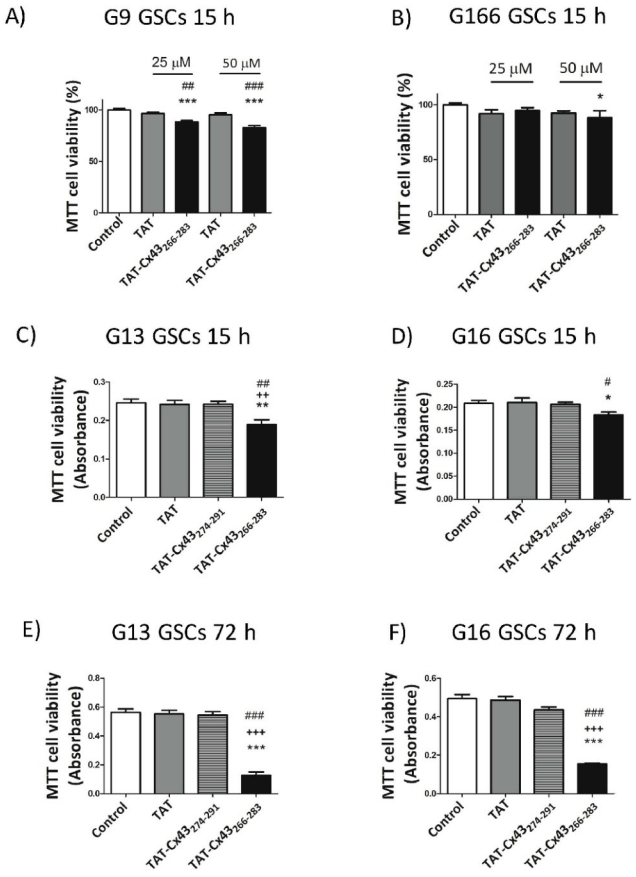

Figure S4. **Effect of TAT-Cx43$_{266-283}$ on primary GSC and G166 GSC viability after 15 and 72h. Related to Figure 5.**

Primary G9 GSCs or G166 GSCs were plated at 5500 cells/cm^2 and incubated with 25 or 50 µM TAT or TAT-Cx43$_{266-283}$ for 15 h **(A, B)**. Primary G13 or G16 GSCs were plated at 5500 cells/cm^2 and incubated with 50 µM TAT, 50 µM TAT-Cx43$_{266-283}$ or TAT-Cx43$_{274-291}$ for 15 h **(C, D)**. Primary G13 or G16 GSCs were plated at 5500 cells/cm^2 and incubated with 50 µM TAT-Cx43$_{266-283}$ or TAT-Cx43$_{274-291}$ for 72 h **(E, F)**. The cell viability was analyzed using a MTT assay as described in the Experimental procedures section. The results are expressed as the percentages of the absorbance found in the control and are the mean ± s.e.m. of 3 experiments (ANOVA ***p<0.001; **p<0.01; *p<0.05; TAT-Cx43$_{266-283}$ vs Control; ###p<0.001; ##p<0.01; #p<0.05, TAT-Cx43$_{266-283}$ vs TAT; +++p<0.001; ++p<0.01; TAT-Cx43$_{266-283}$ vs TAT-Cx43$_{274-291}$).

Movies S1-S3. Effect of TAT-Cx43$_{266-283}$ on primary G9 GSC motility. Related to Figure 3.

Primary G9 GSCs plated at a low density were incubated in the absence (Control; **S1**) or presence of 50 μM TAT **(S2)** or 50 μM TAT-Cx43$_{266-283}$ **(S3)**. Phase-contrast time-lapse movies show the random movement of primary G9 GSCs. Images were acquired for 12 h at 10 min intervals as described in the Experimental procedures section. Note the reduction in the motility of primary G9 GSCs promoted by TAT-Cx43$_{266-283}$. Frame size= 480 x 360 pixels. Frame rate= 10 frames per second.

Movies S4-S9. Effect of TAT-Cx43$_{266-283}$ on G9, G13 and G16 explants. Related to Figure 6.

Tumor explants plated immediately after surgery were incubated in the presence of 100 μM TAT **(S4, S6, S8)** or 100 μM TAT-Cx43$_{266-283}$ **(S5, S7, S9)**. Phase-contrast time-lapse movies showing the spread and growth of cells from the tumor blocks (**S4** and **S5** for G9; **S6** and **S7** for G13; **S8** and **S9** for G16, respectively). Images were acquired for the indicated times at 10 min intervals as described in the Experimental procedures section. Note the reduction in the survival, migration and growth of glioblastoma cells promoted by TAT-Cx43$_{266-283}$. Frame size= 480 x 360 pixels. Frame rate= 15 frames per second.